Effects of Load Ratio and Temperature on the Near-Threshold Fatigue Crack Propagation Behavior in a CrMoV Steel

P. K. LIAW, A. SAXENA, V. P. SWAMINATHAN, and T. T. SHIH

The influence of temperature in the range of 24 to 260 °C and load ratio on the near-threshold fatigue crack growth rate behavior of a CrMoV steel was characterized. At all temperatures investigated, the threshold stress intensity range, ΔK_{th}, for fatigue crack growth decreased with increasing load ratio. The near-threshold crack growth rates increased significantly at 149 °C when compared with the rates at room temperature. However, the crack growth rates at 260 °C were comparable to those at 149 °C. These observations are rationalized in terms of the concepts of roughness and oxide-induced crack closure. Extensive fracture surface characterization using SEM, oxide thickness measurements by Auger spectroscopy, and roughness measurements by light-section-microscopy were conducted to substantiate the explanations.

I. INTRODUCTION

IN order to predict the life of a component subjected to high frequency gravity bending or flow-induced vibrations, fatigue crack growth rate (FCGR) data are needed in the near-threshold region. The FCGR behavior at the threshold level is strongly influenced by variables such as microstructure, load ratio (R = ratio of the minimum to maximum load) and environment (including temperature).[1-21]

In this study, the influence of load ratio (in the range of 0.1 to 0.8) and temperature (in the range of 24 to 260 °C) on the near-threshold FCGR behavior of a forged CrMoV steel (ASTM A470 Class 8) is characterized. In order to allow accurate interpolation of the effects of load ratio and temperature for conditions other than for which data are available, it is necessary to develop an understanding of the mechanisms by which these variables influence the near-threshold FCGR behavior. Therefore, extensive fracture morphology characterization, measurements of residual oxide layer thicknesses on the fracture surfaces by Auger spectroscopy, and surface roughness measurements by light-section-microscopy were included as a part of this study.

The concept of crack closure has been used to rationalize the influence of loading, environmental and microstructural variables on the near-threshold FCGR behavior in several alloying systems.[1-25] Thus, we have performed crack closure measurements during the course of the FCGR testing. The present experimental results and observations are discussed in light of the crack closure concept.

II. EXPERIMENTAL PROCEDURE

A. *Material and Specimens*

The material investigated was a forged ASTM A470 Class 8, CrMoV steel. The chemical composition of this steel in weight percent was 0.32 C, 0.78 Mn, 0.28 Si, 1.20 Cr, 1.18 Mo, 0.23 V, 0.012 P, 0.011 S, 0.13 Ni, 0.05 Cu, 0.005 Al, 0.010 Sn, 0.008 As, and balance Fe. The mechanical properties are shown in Table I. The material was austenitized at 950 °C, air cooled, and tempered at 680 °C. The steel has a bainitic microstructure with an average prior austenite grain size of approximately 35 μm. Compact type (CT) specimens, 50.8 mm wide, 60.9 mm high, and 12.7 mm thick, were used to develop the near-threshold FCGR data. Prior to testing, all specimens were precracked in accordance with the ASTM standard E647-81.

B. *Fatigue Crack Growth Rate Testing*

The testing temperatures were 24 °C, 149 °C, and 260 °C, and the environment was laboratory air. Heating tapes were wrapped around the specimens to obtain the desired temperature. A thermocouple mounted near the test section of the specimen surface was used to control and monitor the temperature. The relative humidity in laboratory air at 24 °C was approximately 40 pct. The load ratios studied were 0.1, 0.3, 0.5, and 0.8. The loading frequency was 100 Hz and the waveform was sinusoidal.

The crack length was determined by the compliance technique using a clip gage mounted on the front face of the specimen. The fatigue crack growth testing was conducted on a computer-controlled, servo-hydraulic fatigue machine. The PDP 11/34 computer interfaced with the machine provided the capability for automatic test control, data acquisition, and data analysis. The details of the automated system have been reported earlier.[19,26] Briefly, the stress intensity range, ΔK, was automatically decreased with crack length, a, according to the following equation, suggested by Saxena, *et al.*[26]

$$\Delta K = \Delta K_0 e^{c(a-a_0)} \qquad [1]$$

Table I. Tensile Properties of ASTM A470 Class 8 Steel

Temp. (°C)	0.2 Pct Yield Strength (MPa)	Ultimate Strength (MPa)	Elongation* (Pct)	Reduction in Area (Pct)
24	623	776	14	39
427	516	625	14	53

*Using 5 cm gage length

P. K. LIAW and A. SAXENA, Senior Engineers, are with Metallurgy Department, Westinghouse Research and Development Center, Pittsburgh, PA 15235, and V. P. SWAMINATHAN and T. T. SHIH, Senior Engineers, are with Steam Turbine-Generator Division.

Manuscript submitted October 14, 1982.

where ΔK_0 and a_0 are initial stress intensity range and crack length, respectively, and c has a value of $-0.118\ mm^{-1}$. Thus, Eq. [1] was used to decrease ΔK for developing near-threshold crack growth rate data.

The crack closure level was measured by the unloading compliance technique.[9,12,17,27] In order to determine accurately the crack closure point, the linear elastic displacement was subtracted from the total displacement in the load *vs* displacement curve. This facilitated the selection of the crack closure point. The details of this procedure are schematically illustrated in Figure 1.

C. *Fracture Surface Characterization*

1. *SEM Characterization*

Scanning electron microscopy was used to characterize the extent of intergranularity on the fracture surfaces of the tested specimens. For measuring the proportion of intergranular cracking, the intergranular facets on the SEM photomicrographs were traced on transparencies. The percentage of intergranular fracture was then calculated by a Quantitative Image Analyzer. At a given value of ΔK which corresponds to a certain crack length on the fracture surface, the average percentage of intergranularity was determined over several photomicrographs across the specimen thickness.

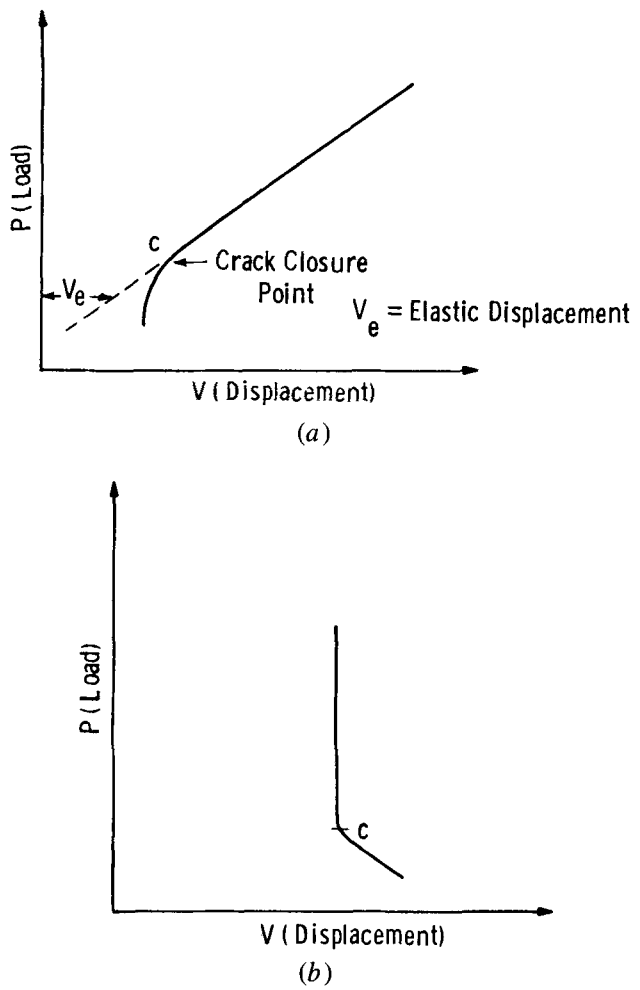

Fig. 1—(*a*) Typical load-displacement curve; (*b*) load-displacement curve after subtracting the unloading linear elastic displacement.

2. *Oxide Thickness Measurements*

Auger spectroscopy was used to measure the thickness of the oxide deposit on the fracture surface. The sputtering rate in the Auger spectrometer was calibrated to a known thickness of tantalum oxide. From previous experience with Fe and Ni base alloys,[28] it is known that the oxides of these metals all sputter at approximately the same rate as tantalum oxide. As the Ar^+ ions sputter the fracture surface, the atomic percents of compositional elements in the oxide can be plotted out. Consequently, a depth profile of oxygen or iron *vs* the average distance from the fracture surface into the oxide can be obtained. The average oxide thickness was defined as the distance where the atomic percent of oxygen is equal to that of iron.[9,29]

3. *Surface Roughness Measurements*

The roughness of the fracture surface was characterized by a light-section microscope. A schematic describing this technique is shown in Figure 2. In this method, a narrow band of light is projected on the fracture surface at an angle of 45 deg and the image is observed on the other 45 deg plane. The image thus obtained closely follows the profile of the fracture surface and allows us to make roughness measurements. For determining the quantitative roughness data corresponding to a value of ΔK, several photographs of roughness profiles were taken across the specimen thickness. In Figure 2, the value of roughness, h, was defined as the average height of the roughness peaks on the various photographs. The average width, w, of the roughness peaks can also be measured (Figure 2).

III. RESULTS

A. *Influence of Load Ratio and Temperature*

The influence of load ratio on near-threshold fatigue crack growth rates in the CrMoV steel is shown in Figures 3(a) to (c) at 24 °C, 149 °C, and 260 °C, respectively. Increasing the R value increases the rates of near-threshold crack propagation at all three temperatures. The influence of R on crack

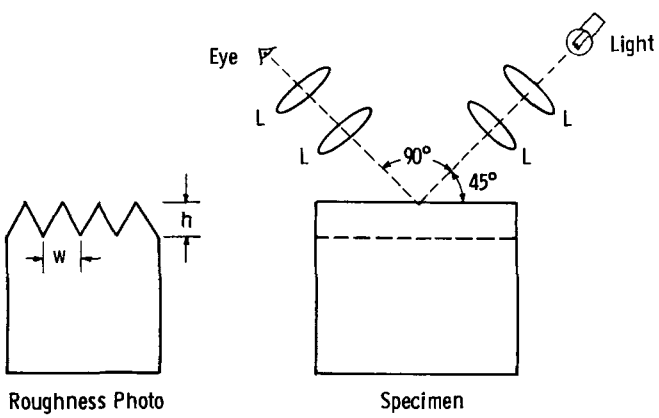

Fig. 2—Schematic of light-section-microscopy.

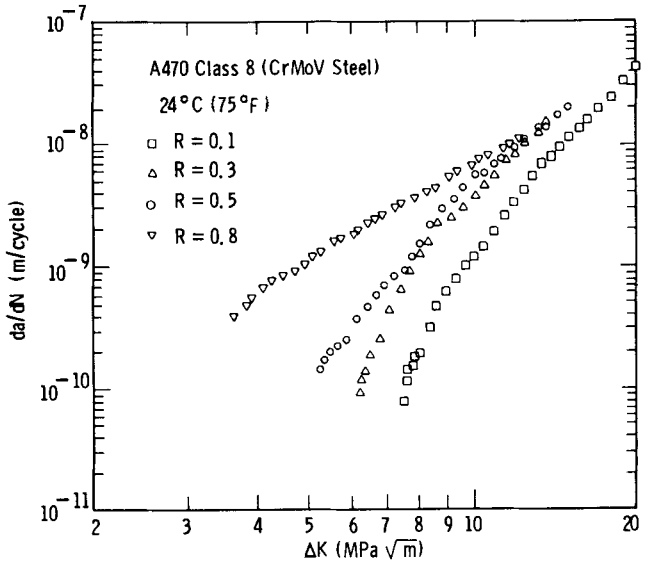

(a)

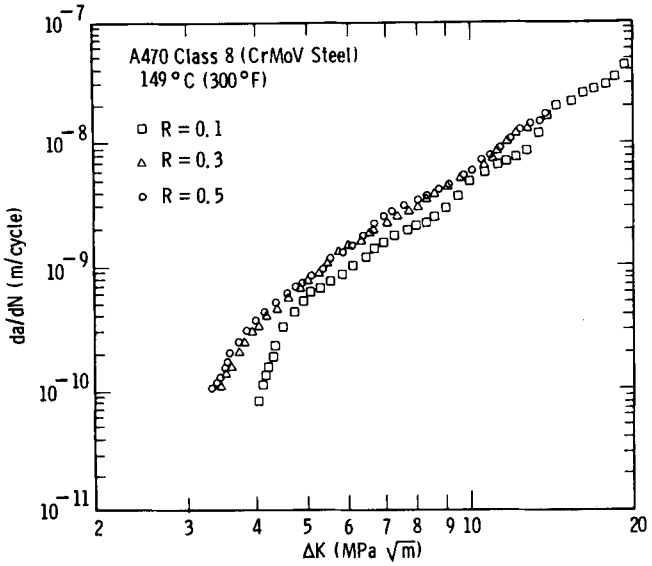

(b)

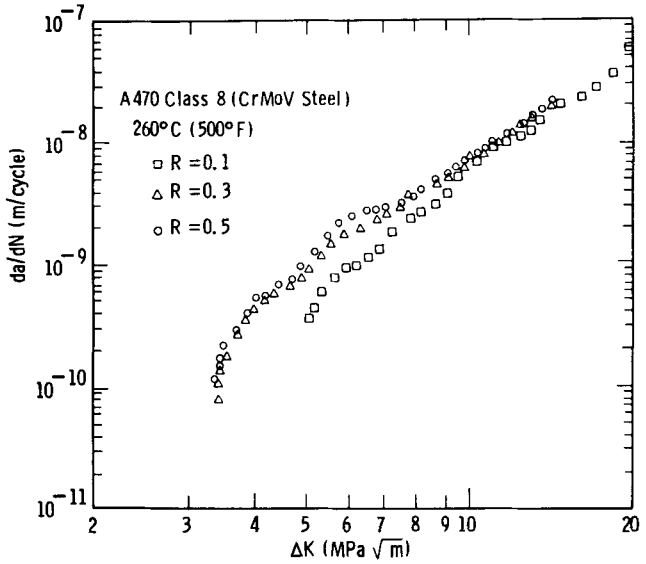

(c)

Fig. 3—(*a*) Effect of load ratio on fatigue crack growth rates at 24 °C, (*b*) effect of load ratio on fatigue crack growth rates at 149 °C, and (*c*) effect of load ratio on fatigue crack growth rates at 260 °C.

growth behavior becomes more significant with the decrease in ΔK (Figures 3(a) to (c)). It appears that increasing the temperature from 24 °C to 149 °C (or 260 °C) reduces the influence of load ratio on crack growth rates. Similar trends were also reported previously by Paris *et al.*[1] in a pressure vessel steel.

At a fixed value of R, increasing the temperature from 24 °C to 149 °C results in significant increases of the near-threshold crack propagation rates (Figures 4(a) and (b)). As the value of ΔK decreases, the effect of temperature on the crack growth rates becomes more pronounced. However, the crack propagation rates at 149 °C and 260 °C are comparable (Figures 4(a) and (b)), and thus, the influence of temperature appears to saturate. This behavior will be discussed later.

To determine the threshold stress intensity range, ΔK_{th}, the crack growth rates smaller than 7×10^{-10} m/cycle were fitted to the equation, $da/dN = b\Delta K^m$, by the least-squares technique. The value of ΔK_{th} was operationally defined as

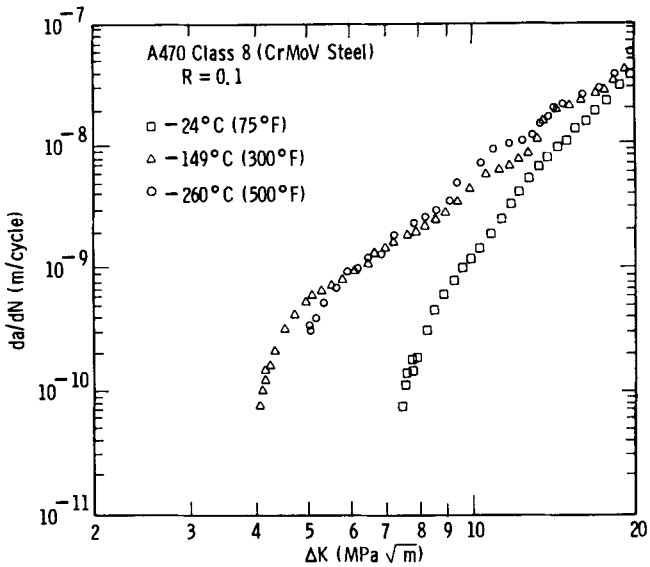

(a)

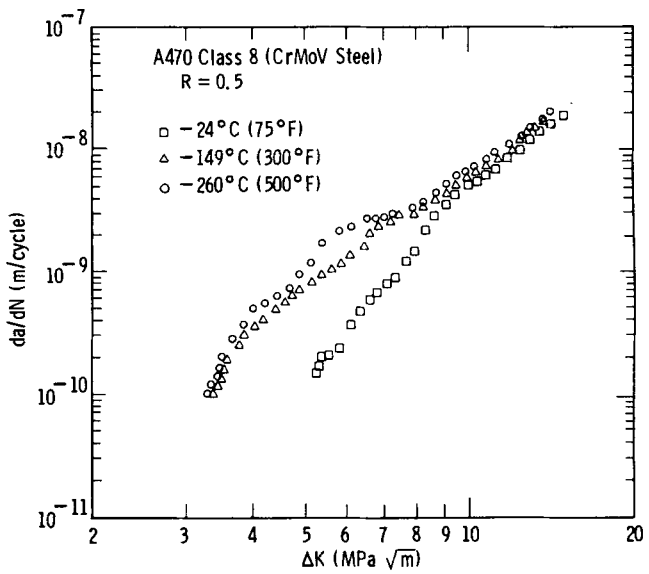

(b)

Fig. 4—(*a*) Effect of temperature on fatigue crack growth rates at R = 0.1; (*b*) effect of temperature on fatigue crack growth rates at R = 0.5.

the stress intensity range corresponding to a propagation rate of 1×10^{-10} m/cycle and was obtained from the fitted equation. Table II lists the values of ΔK_{th} at various temperatures and R values. Figure 5 summarizes the influence of load ratio and temperature on threshold crack propagation behavior in the CrMoV steel. At the three temperatures investigated, increasing R decreases the values of ΔK_{th}. However, the dependence of ΔK_{th} on load ratio at 24 °C is larger than that at 149 °C and 260 °C. At low values of R, ΔK_{th} at 24 °C is larger than that at 149 °C or 260 °C. By comparison, the difference in the values of ΔK_{th} at 24 °C and 149 °C (260 °C) is significantly less at higher values of R. Similar results were previously reported in other steels.[1]

For engineering applications, the growth rates larger than 10^{-9} m/cycle (Paris Region) were fitted to the earlier-mentioned equation. The values of b and m for this region of FCGR behavior, which are different from those in the near-threshold region, are listed in Table II.

B. *Fracture Morphology*

At 24 °C, fracture morphology changes with the value of ΔK (Figure 6(a)). A plot of percent intergranular fracture as a function of ΔK is shown in Figure 7 for the three load ratios at which data were obtained at room temperature. As ΔK increases from the threshold value, the percent intergranular fracture increases, reaches a maximum, and then decreases at the three load ratios. It was noted that the value of ΔK corresponding to the maximum intergranularity was nearly the same for all three load ratios. At a given value of ΔK, increasing R appears to decrease the percent intergranularity. Similar data have been previously reported for other steels.[9,30,31] However, the fracture at 149 °C and 260 °C is completely transgranular regardless of ΔK and R values, as indicated by a few examples given in Figure 6(b).

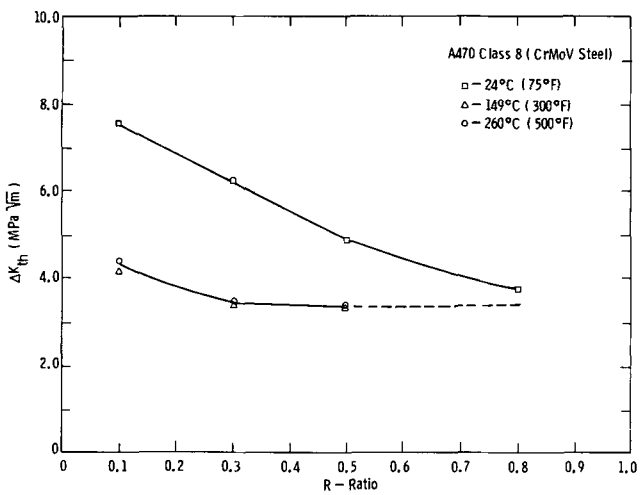

Fig. 5—Effects of load ratio and temperature on ΔK_{th}.

C. *Crack Closure Measurements*

Elber[22,23] had proposed that the driving force for the growth of a fatigue crack was the effective stress intensity range, ΔK_{eff}. He argued that a zone of residual deformation left in the wake of a growing fatigue crack caused the crack to remain closed during a portion of the loading cycle. This portion of the loading cycle was ineffective in growing the crack and should be disregarded in calculating the driving force. Hence, he defined $\Delta K_{eff} = K_{max} - K_{cl}$ where K_{cl} was the stress intensity level corresponding to the measured closure load. Recently, several studies[1-18,20] have been published, which show that crack closure takes on added significance in the near-threshold region because additional factors, such as oxide deposits and the roughness of the fracture surfaces, cause high closure loads. Thus, an attempt was made in this study to measure the closure loads and plot the crack growth behavior in terms of ΔK_{eff}.

In Figures 8(a) and (b), the crack growth rate data of Figures 3(a) and (c) are plotted against ΔK_{eff} for $R = 0.1$, 0.3, 0.5, and 0.8 at temperatures of 24 °C and 260 °C, respectively. At both temperatures, the difference in the fatigue crack growth behavior at various R values is considerably reduced when the data are expressed in terms of ΔK_{eff}. Similar results were reported previously.[8,9,20,32-34] In Figure 8(c), the crack growth rate behavior for R of 0.1 at 24 °C and 260 °C is plotted. The large difference in the near-threshold crack growth behavior at these temperatures, shown earlier in Figure 4(a), appears to have been reconciled. Further, Figure 8(d) summarizes the da/dN *vs* ΔK_{eff} behavior at selected load ratios and temperatures covering the entire range of these values for which tests were done. Trend lines are used instead of data points for clarity. All data appear to converge in a narrow band. Thus, it suggests that the influence of R and temperature on the rates of near-threshold crack growth can be rationalized by the

Table II. Parameters for Characterizing Fatigue Crack Growth Rates

Temperature (°C)	R	ΔK_{th} (MPa $\sqrt{m}$)	Near-Threshold Region		Paris Region	
			m*	b*	m*	b*
24	0.1	7.55	12.4	1.41×10^{-21}	5.21	7.53×10^{-15}
24	0.3	6.25	11.4	8.36×10^{-20}	4.87	4.80×10^{-14}
24	0.5	4.90	5.42	1.91×10^{-14}	4.31	1.99×10^{-13}
24	0.8	3.64**	4.39	1.31×10^{-12}	2.59	1.67×10^{-11}
149	0.1	4.10	12.1	3.75×10^{-18}	3.26	2.50×10^{-12}
149	0.3	3.35	6.27	5.22×10^{-14}	2.87	7.76×10^{-12}
149	0.5	3.35	6.78	2.82×10^{-14}	2.95	6.79×10^{-12}
260	0.1	4.40	8.00	7.21×10^{-16}	3.37	2.17×10^{-12}
260	0.3	3.45	11.0	1.28×10^{-16}	2.93	7.86×10^{-12}
260	0.5	3.40	10.4	3.13×10^{-16}	2.71	1.34×10^{-11}

*$da/dN = b\Delta K^m$. The units of da/dN and ΔK are m/cycle and MPa $\sqrt{m}$, respectively.
**The lowest ΔK value in Figure 3(a).

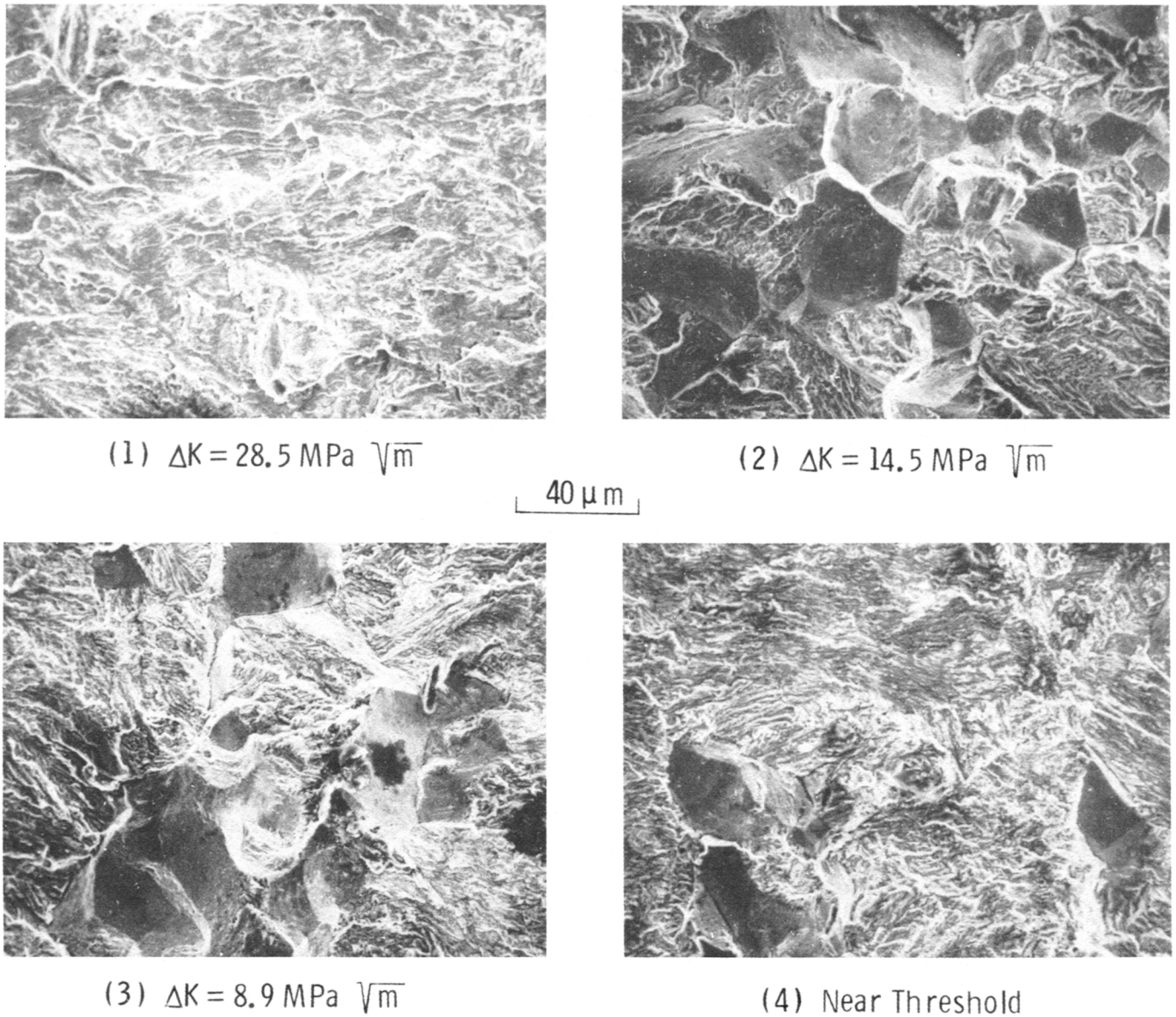

(*a*)

Fig. 6—(*a*) Fracture morphology at 24 °C at $R = 0.1$.

crack closure model. It should be noted that at threshold, the crack closure level at 24 °C is higher than that at 260 °C (Table III).

D. *Measurements of Oxide Thickness and Surface Roughness*

The results from oxide thickness measurements at threshold are presented in Figure 9. For a given R, increasing the temperature results in a thicker oxide layer.

The values of surface roughness at threshold and at various load ratios, determined by the light-section-microscopy, are shown in Figure 10(a). The surface roughness at threshold decreases with an increase in temperature (Figure 10(a)). Also, the surface roughness at threshold remains unaffected by the load ratio. Similar behavior was previously reported on pearlitic steels.[13]

The surface roughness behavior was investigated at various ΔK levels. The results are shown in Figure 10(b). The trend of decreasing surface roughness with increasing temperature, as noted at threshold, is also observed at other ΔK values. There is a tendency for surface roughness to increase approximately linearly with ΔK with the following exception. At 24 °C, there is a region of ΔK in which the surface roughness is higher than would be expected from the linear trend exhibited by the overall data. This behavior is discussed further in the next section.

IV. DISCUSSION

The data presented in the previous section strongly suggest that crack closure plays an important role in the near-threshold fatigue crack growth behavior. The influence of

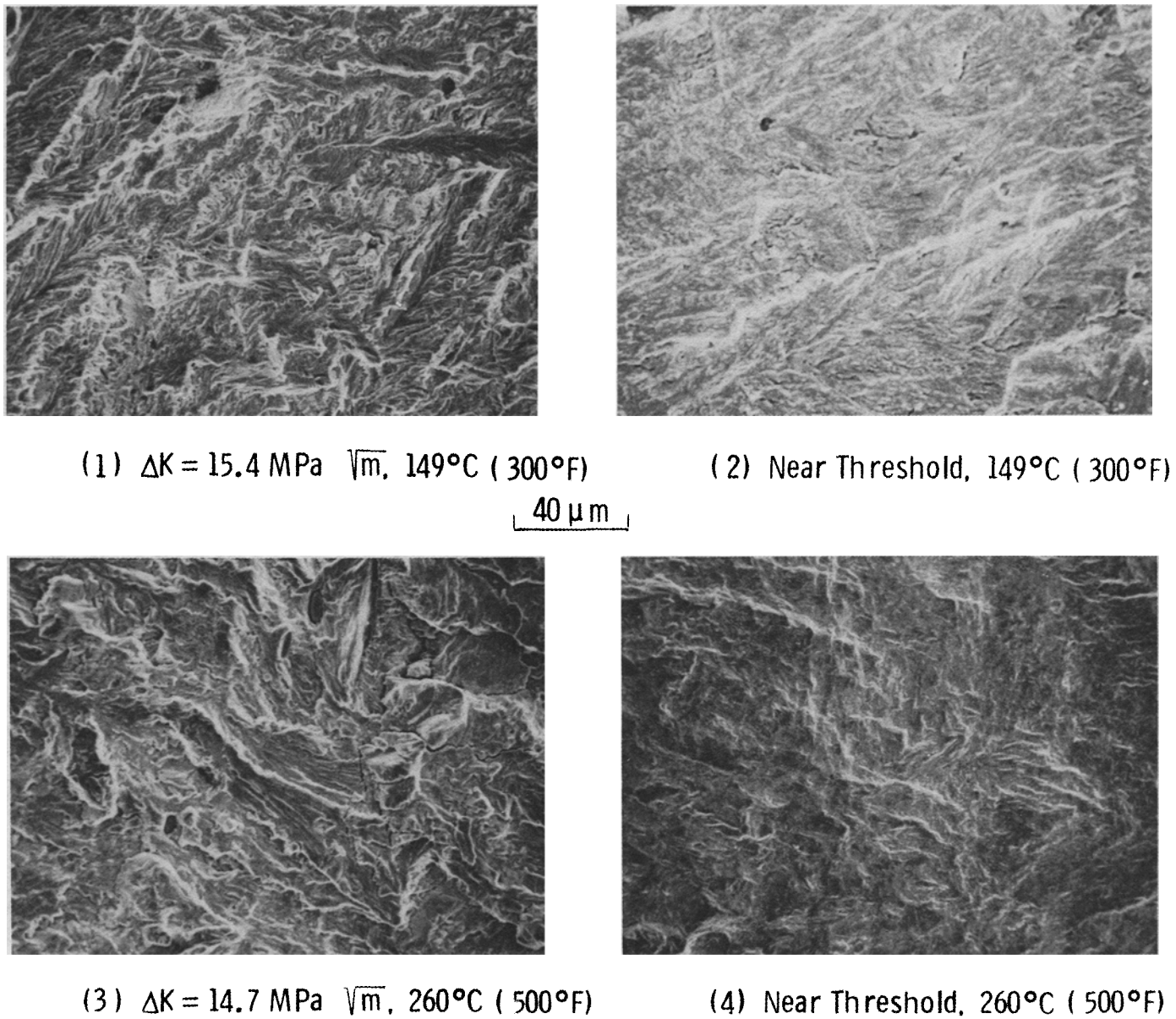

(*b*)

Fig. 6— (*b*) fracture morphology at 149 °C and 260 °C for $R = 0.1$.

both load ratio and temperature is reconciled when the da/dN results are plotted as a function of ΔK_{eff}. Therefore, we will critically evaluate the role of crack closure in the near-threshold region.

A. *Mechanisms of Crack Closure*

Elber's[22,23] concept of crack closure (sometimes referred to as plasticity-induced crack closure)[3–6] has been mentioned earlier. In addition to the plasticity-induced crack closure, two other forms of crack closure are significant in the threshold region.[3–6,20] They are the oxide-induced closure and the surface roughness-induced closure. Both mechanisms are briefly described.

It has been observed[5,6,7,20] that in air or in oxygen-containing environments, thick layers of oxide form on the fracture surfaces in the near-threshold region in steel and copper specimens. The formation of oxide is enhanced by the fretting between the mating fracture surfaces due to plasticity-induced crack closure.[3–6,9,20] In this investigation, thermal oxidation at 149 °C and 260 °C may also contribute to the formation of oxide deposits, thereby resulting in thicker oxide layers than at 24 °C (Figure 9). These oxide layers tend to wedge the crack tip and cause the cracks to close at loads significantly larger than the applied minimum load, thus resulting in values of ΔK_{eff} which are much lower than ΔK.

In some alloying systems, the crack growth in the near-threshold region follows a more crystallographic path within a grain than the crack growth at higher ΔK values. This implies that the crack tip is often at an angle other than 90 deg to the direction of loading which results in significant Mode II displacements[5,11,24] in the crack tip region. In turn, the Mode II displacements cause a mismatch between the mating fracture surfaces, which promotes an early contact between the fracture surfaces and provides another mechanism of crack closure. This form of crack closure is

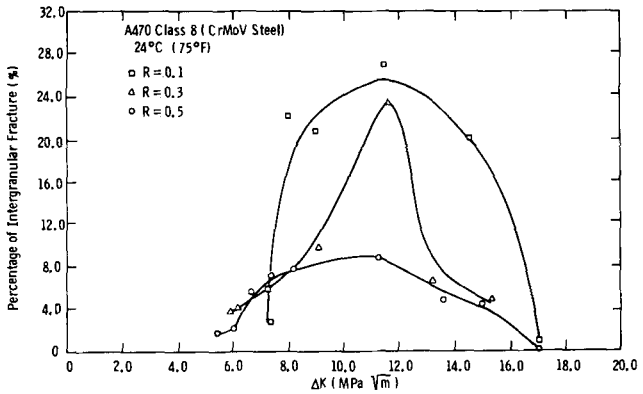

Fig. 7—Effects of load ratio and ΔK on intergranular fracture at 24 °C.

referred to as surface roughness-induced crack closure[5,6,11] because the extent of mismatch is directly dependent on the roughness of the fracture surface.

We are now ready to discuss the present experimental results and determine which particular crack closure mechanism governs the near-threshold crack growth behavior in CrMoV steel in the temperature range of 24 °C to 260 °C.

B. *Effect of Oxide Layer on Crack Closure*

Table IV gives the values of oxide layer thickness and cyclic crack tip opening displacement (CTOD) at threshold for load ratios and temperatures investigated. The values of CTOD were calculated using the equation,[3] CTOD $= 0.49(\Delta K_{th}^2)/(2\sigma_y E)$, where σ_y is yield strength

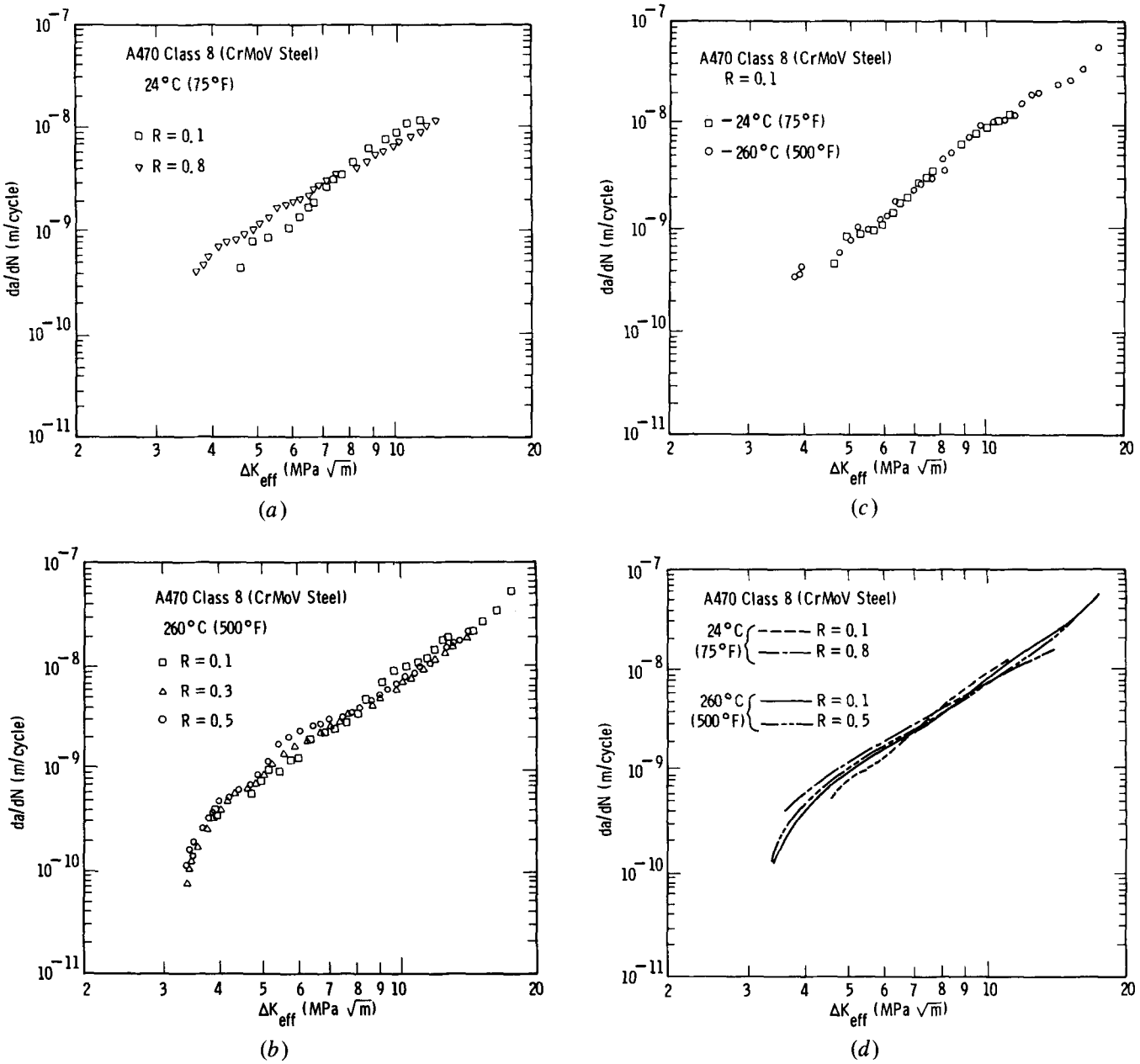

Fig. 8—(*a*) Fatigue crack growth rate as a function of ΔK_{eff} at 24 °C, (*b*) fatigue crack growth rate as a function of ΔK_{eff} at 260 °C, (*c*) fatigue crack growth rate as a function of ΔK_{eff} at $R = 0.1$ and at two temperatures, and (*d*) plots of ΔK_{eff} *vs* da/dN trends at two temperatures and at three R values.

Table III. Crack Closure Level at Threshold and at $R = 0.1$

Temperature (°C)	K_{cl} (MPa $\sqrt{m}$)
24	3.4
260	1.3

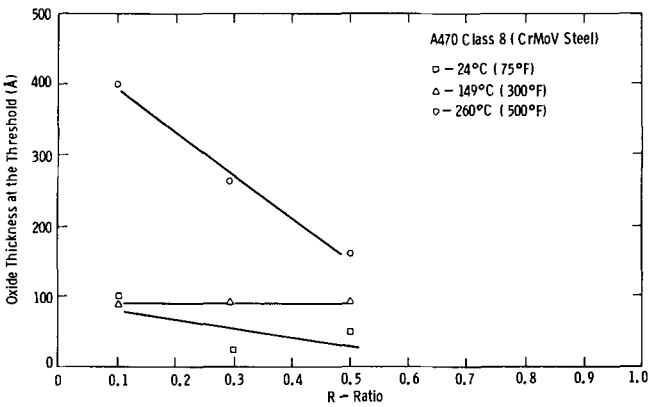

Fig. 9—Results of oxide thickness measurements.

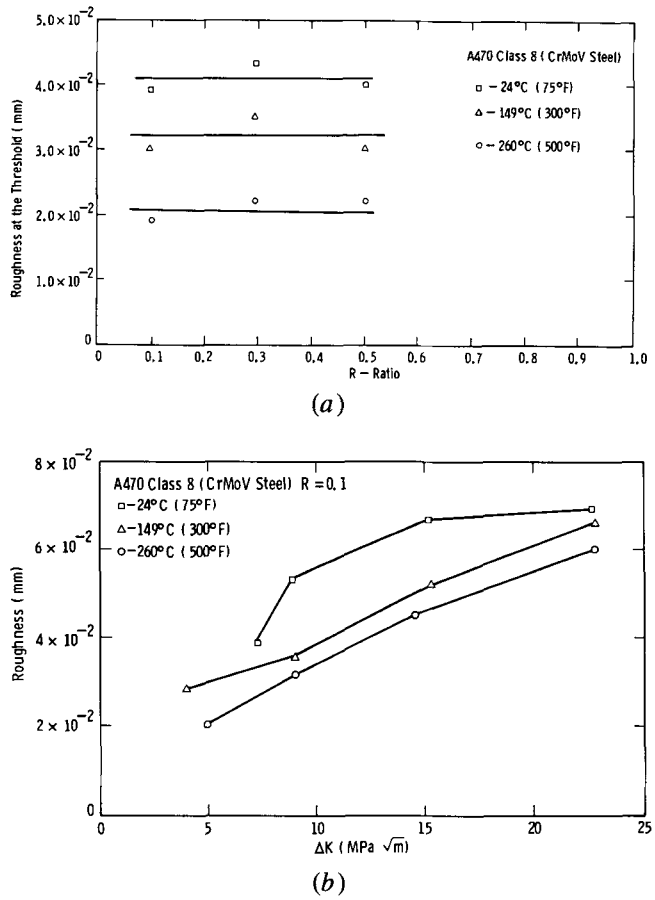

Fig. 10—(*a*) Results of roughness measurements at the threshold; (*b*) results of roughness measurements at various ΔK values.

and E is Young's modulus. A comparison between oxide layer thickness and cylic CTOD may give a qualitative estimate of the extent to which wedging may occur at the crack tip. If the cyclic CTOD values are much larger than oxide layer thickness, the presence of oxide is not expected to be a factor in affecting the near-threshold behavior, as observed at 24 °C and 149 °C for all load ratios (Table IV). However, at 260 °C the oxide layer thicknesses are comparable to cyclic CTOD levels (Table IV). When the oxide layer thickness becomes comparable to cyclic CTOD, it can be argued that at low R values (<0.5), the threshold may be influenced by oxide wedging of the crack tip.[3-6,20] However, at high R values, the cyclic CTOD is superimposed on a high mean level of crack opening displacement; hence, the oxide layer (even though comparable in thickness with the cyclic CTOD level) may not contribute significantly to crack closure. It was reported[3] that in air environments and at low load ratios, thick layers of oxide (~0.2 μm) formed on the fracture surfaces of 2.25Cr-1Mo steels and promoted crack closure. In contrast, in our tests the oxide layers were considerably thinner ($\leq$0.04 μm), which would indicate that oxide-induced crack closure might not be the only controlling factor in 260 °C testing. Therefore, alternate mechanisms, such as surface roughness-induced crack closure, should be considered.

Table IV. Oxide Thickness, Fracture Surface Roughness, and Crack Tip Opening Displacement at Threshold

Temp. (°C)	R	Oxide Thickness (Å)	Surface Roughness (Å)	Cyclic Crack Tip Opening Displacement (CTOD)* (Å)
24	0.1	96	39×10^4	1137
24	0.3	25	43×10^4	769
24	0.5	47	30×10^4	473
149	0.1	87	30×10^4	362
149	0.3	90	35×10^4	242
149	0.5	91	30×10^4	241
260	0.1	400	19×10^4	418
260	0.3	264	22×10^4	256
260	0.5	160	29×10^4	249

*CTOD = $0.49(\Delta K_{th}^2)/(2\sigma_y E)$.

C. *Effect of Surface Roughness on Crack Closure*

Values of fracture surface roughness at threshold are listed in Table IV. These values are much larger (approximately two to four orders of magnitude) than the corresponding oxide layer thicknesses and cyclic CTOD values. Note that the values of surface roughness are comparable with the average prior austenite grain size. As discussed earlier, in the presence of any Mode II displacements in the crack tip region, these high levels of surface roughness are likely to cause large contributions to crack closure. Recently, Suresh and Ritchie[6] have proposed the following expression for estimating the stress intensity level at closure, K_{cl}, as a function of the surface roughness and the extent of Mode II displacements.

$$\frac{K_{cl}}{K_{max}} = \sqrt{\frac{2\delta x}{1 + 2\delta x}} \qquad [2]$$

$$(\delta = h/w; \quad x = u_{II}/u_I)$$

where u_I and u_{II} are the Mode I and Mode II displacements, respectively. Substituting in Eq. [2] the measured values of $h/w = 0.13$ and 0.06 at 24 °C and 260 °C, respectively, and

the appropriate K_{cl}/K_{max} values from Table III, we estimate the values of x as 0.73 and 0.67 at the respective temperatures. These values of x imply significant Mode II displacements. Moreover, these values are qualitatively in agreement with the experimental measurements of Davidson[24] who used a stereo-imaging technique to demonstrate that the magnitude of the Mode II displacement in the threshold region is a significant fraction of the Mode I displacement in a low carbon steel.

The surface roughness at threshold is independent of the load ratio, R, at all three temperatures (Figure 10(a)). However, the same roughness level is expected to cause a more significant extent of crack closure at low R values than at high R values,[6] since there is a higher mean load and a possibly smaller fraction of Mode II displacements,[24] x, with increasing R values. The larger extent of crack closure at lower load ratios reduce ΔK_{eff} more significantly than at high load ratios. Therefore, the crack growth rate in the near-threshold region is expected to decrease with a decrease in R, which is in agreement with the experimental results. Hence, the influence of R on the near-threshold behavior can be explained by the surface roughness-induced crack closure mechanism.

The influence of temperature on the near-threshold fatigue crack growth behavior in CrMoV steel can also be explained on the basis of surface roughness and oxide layer thickness measurements. The surface roughness decreases with an increase in temperature (Figures 10(a) and (b)). Hence, it may be deduced that decreasing the temperature increases the roughness-induced crack closure level (provided that the fraction of the Mode II displacement, x, remains relatively insensitive to the temperatures investigated, which is a reasonable assumption based on the calculated values of x, 0.73 and 0.67, at 24 °C and 260 °C, respectively) and thus, reduces near-threshold crack propagation rates which is in general agreement with the experimental results in Table III and Figures 4 and 5. However, it was observed that the difference in the fatigue crack growth behavior at 149 °C and 260 °C was only marginal. This may be related to the presence of thicker oxide layers at 260 °C than at 149 °C. The thicker oxide layer at 260 °C will tend to offset the influence of lower surface roughness and therefore, the resulting crack growth rates can be comparable to those obtained at 149 °C. Increasing the load ratio generally reduces the contribution of roughness-induced crack closure, as reported before. Consequently, increasing R decreases the difference in the values of ΔK_{th} at 24 °C and 149 °C (260 °C) (Figure 5). Furthermore, the greater influence of load ratio on near-threshold crack propagation behavior at 24 °C than at 149 °C (260 °C) (Figures 3 and 5) may result from the more significant roughness-induced crack closure at 24 °C (Figures 10(a) and (b)).

In Figure 10(b), we have plotted the measured values of surface roughness with ΔK. There is a general tendency for the roughness to increase with increasing ΔK. This may be due to higher amounts of plasticity associated with crack growth rates at higher ΔK levels. Also, an interesting trend is presented by the curve corresponding to 24 °C which merits further discussion. In the region of ΔK at 24 °C (from approximately 8 to 14 MPa $\sqrt{m}$) where intergranular fracture was significant (Figure 7), the surface roughness was higher than expected from the general linear trend exhibited by the overall data, as mentioned before (Figure 10(b)). It is suggested that the higher roughness level at 24 °C than at 149 °C or 260 °C may be related to the presence of intergranularity. The above observations imply that microscopic phenomena accompanying fatigue crack growth in the near-threshold region can influence the fracture surface roughness, and thereby affect the crack growth rates. Similar fracture-surface-roughness-based explanation has been offered by Gray *et al.*[13,14] to rationalize the influence of grain size on the near-threshold fatigue crack growth behavior in pearlitic steels. Minakawa *et al.*[10,11,12] have proposed that in AISI 1018 steels, the duplex microstructure containing martensite encapsulated volumes of ferrite gives a rougher fracture surface than observed for the normalized microstructure. This causes the crack growth rates in the near-threshold region to be slower for the duplex structure steels. The common observation in all these studies and ours appears to be that several microstructural variables influence the near-threshold fatigue crack growth rate behavior by affecting the roughness characteristics of the fracture surfaces in the wake of the crack.

Another aspect of our results which merits discussion is the role of moisture. The relative humidity at room temperature in a controlled laboratory environment is approximately 40 pct. At 149 °C and 260 °C, the relative humidity levels are much lower than that at 24 °C. We feel that the intergranular fracture observed at room temperature may have been due to the hydrogen embrittlement caused by the presence of moisture.[35] However, the influence of the apparent hydrogen embrittlement on the near-threshold behavior is to increase the crack growth rate. Unless rationalized in terms of surface roughness-induced crack closure, the expected crack growth behavior may be quite opposite to the experimental results at the three temperatures investigated. Thus, it suggests that at 24 °C, roughness-induced crack closure may outgrow the influence of moisture in near-threshold crack propagation, which results in slower rates of crack growth, compared to the data at 149 °C and 260 °C. As mentioned before, the maximum intergranularity at 24 °C occurs at a ΔK of about 10.8 MPa $\sqrt{m}$ regardless of R values (Figure 7). Interestingly, at the maximum intergranularity, the corresponding cyclic plastic zone size[36] of 36 μm $[= (\pi/32)(\Delta K/\sigma_y)^2]$ is approximately equal to the prior austenite grain size. Similar behavior was observed in other steels.[9,30,31]

A pertinent question that may be asked is 'what is the role of surface roughness at high ΔK values?' This question can be readily answered by noting that Mode II displacements at higher ΔK levels are significantly lower.[6,10–12,24,25] Hence, at higher ΔK values the surface roughness contribution to K_{cl} will be considerably reduced using Eq. [2], even though surface roughness increases with increasing ΔK (Figure 10(b)). Consequently, increasing ΔK levels reduces the influence of roughness-induced crack closure, thereby resulting in less dependence of fatigue crack propagation rates on load ratio and temperature at higher ΔK values (Figures 3 and 4).

From the above discussion it is clear that the near-threshold fatigue crack growth behavior and the influence of loading and environmental variables depend on several synergestic factors such as plasticity, surface roughness, oxide build-up, and hydrogen embrittlement.[3,4,9,20,31] It is difficult

to separate quantitatively the contribution of each of these factors. Therefore, some speculations are involved in rationalizing the results. More experiments, *e.g.*, measurements of Mode I and Mode II displacements, and near-threshold fatigue crack growth testing in inert environments, are needed to further the understanding of threshold crack propagation behavior. Hence, until more experimental evidence is available, the arguments and explanations can thrive only on self-consistency.

V. CONCLUSIONS

1. In CrMoV steel, increasing load ratio decreases the resistance to near-threshold fatigue crack propagation at 24 °C, 149 °C, and 260 °C. However, the influence of R decreases with an increase in temperature.
2. At a given value of R, increasing the temperature from 24 °C to 149 °C significantly increases the rates of near-threshold crack propagation. The effect of temperature appears to saturate above 149 °C. Further, the influence of temperature decreases with an increase in load ratio.
3. At 24 °C, the fracture morphology is a mixture of intergranular and transgranular fracture modes. The percentage of intergranular fracture increases with an increase in ΔK, reaches a maximum, and then decreases. The maximum intergranularity occurs at a ΔK value of approximately 10.8 MPa $\sqrt{m}$ regardless of load ratio. At 149 °C and 260 °C, the fracture morphology is transgranular irrespective of ΔK and R values.
4. During near-threshold crack growth in CrMoV steel, roughness-induced crack closure appears to play a more important role than oxide-induced crack closure. The effects of load ratio and temperature on near-threshold crack propagation behavior are rationalized in terms of the surface roughness-induced crack closure mechanism.

ACKNOWLEDGMENTS

The authors would like to thank W. G. Clark, Jr. and J. Wells for the reviews of the manuscript. Valuable discussions with J. Schreurs are appreciated. We are grateful to M. G. Peck, D. Detar, A. Karanovich, and J. Yex for their assistance in conducting the experiments. The discussions with Professor R. O. Ritchie, Professor M. E. Fine, and Professor A. W. Thompson are also acknowledged. Financial support of the work was provided by the Steam Turbine–Generator Division of the Westinghouse Electric Corporation.

REFERENCES

1. P. C. Paris, R. J. Bucci, E. T. Wessel, W. G. Clark, and T. R. Mager: in *Stress Analysis and Growth of Cracks*, ASTM STP 513, 1972, p. 141.
2. R. J. Bucci, W. G. Clark, and P. C. Paris: in *Stress Analysis and Growth of Cracks*, ASTM STP 513, 1972, p. 177.
3. S. Suresh, G. F. Zamiski, and R. O. Ritchie: *Metall. Trans. A*, 1981, vol. 12A, p. 1435.
4. R. O. Ritchie: *Fatigue Thresholds, Proceedings 1st Intl. Conf.*, Stockholm, J. Backlund, A. Blom, and C. J. Beevers, eds., EMAS Publ. Ltd., Warley, U. K., 1982, p. 503.
5. R. O. Ritchie and S. Suresh: *Metall. Trans. A*, 1982, vol. 13A, p. 937.
6. S. Suresh and R. O. Ritchie: *Metall. Trans. A*, 1982, vol. 13A, p. 1627.
7. A. T. Stewart: *Eng. Fract. Mech.*, 1980, vol. 13, p. 463.
8. Y. Nakai, K. Tanaka, and T. Nakanishi: *Eng. Fract. Mech.*, 1981, vol. 15, p. 291.
9. P. K. Liaw, S. J. Hudak, Jr., and J. K. Donald: *Metall. Trans. A*, 1982, vol. 13A, p. 1633.
10. K. Minakawa and A. J. McEvily: *Fatigue Thresholds, Proceedings 1st Intl. Conf.*, Stockholm, J. Backlund, A. Blom, and C. J. Beevers, eds., EMAS Publ. Ltd., Warley, U. K., 1982, p. 373.
11. K. Minakawa and A. J. McEvily: *Scripta Met.*, 1981, vol. 15, p. 633.
12. K. Minakawa, Y. Matsuo, and A. J. McEvily: *Metall. Trans. A*, 1982, vol. 13A, p. 439.
13. G. T. Gray: Ph.D. Thesis, Carnegie-Mellon University, Pittsburgh, PA, 1981.
14. G. T. Gray, A. W. Thompson, J. C. Williams, and D. H. Stone: *Fatigue Thresholds, Proceedings 1st Intl. Conf.*, Stockholm, J. Backlund, A. Blom, and C. J. Beevers, eds., EMAS Publ. Ltd., Warley, U. K., 1982, p. 345.
15. N. Walker and C. J. Beevers: *Fat. Eng. Mat. Struct.*, 1979, vol. 1, p. 135.
16. I. C. Mayes and T. J. Baker: *Fat. Eng. Mat. Struct.*, 1981, vol. 4, p. 79.
17. R. J. Asaro, L. Hermann, and J. M. Baik: *Metall. Trans. A*, 1981, vol. 12A, p. 1135.
18. J. K. Musuva and J. C. Radon: *Advances in Fracture Research, 5th International Conference on Fracture*, Cannes, France, Pergamon Press, 1981, vol. 3, p. 1365.
19. R. S. Williams, P. K. Liaw, M. G. Peck, and T. R. Leax: *Eng. Fract. Mech.*, in press.
20. P. K. Liaw, T. R. Leax, R. S. Williams, and M. G. Peck: *Acta Met.*, 1982, vol. 30, p. 2071.
21. J. Mckittrick, P. K. Liaw, S. I. Kwun, and M. E. Fine: *Metall. Trans. A*, 1981, vol. 12A, p. 1535.
22. W. Elber: *Eng. Fract. Mech.*, 1970, vol. 2, p. 37.
23. W. Elber: in *Damage Tolerance in Aircraft Structures*, ASTM STP 486, 1971, p. 230.
24. D. L. Davidson: *Fat. Eng. Mat. Struct.*, 1980, vol. 3, p. 229.
25. A. Otsuka, K. Mori, and T. Miyata: *Eng. Fract. Mech.*, 1975, vol. 7, p. 429.
26. A. Saxena, S. J. Hudak, Jr., J. K. Donald, and D. W. Schmidt: *J. of Testing and Evaluation*, 1978, vol. 6, p. 167.
27. M. Kikukawa, M. Jona, and K. Tanaka: *Proceedings of the Second International Conf. on Mechanical Behavior of Materials*, N. Promisel and V. Weiss, eds., Boston, MA, ASM, Metals Park, OH, 1976, p. 716.
28. N. Pessall, M. Baron, J. Schreurs, and J. B. P. Williamson: in *Ion Implantation into Metals*, V. Ashworth, W. A. Grant, and R. P. M. Proctor, eds., Pergamon Press, 1982, p. 55.
29. C. S. White: S. B. Thesis, Massachusetts Institute of Technology, May 1980.
30. R. J. Cooke, P. E. Irving, G. S. Booth, and C. J. Beevers: *Eng. Fract. Mech.*, 1975, vol. 7, p. 69.
31. P. K. Liaw, S. J. Hudak, Jr., and J. K. Donald: *Proceedings of 14th National Symposium on Fracture Mechanics*, ASTM STP 791, in press.
32. R. A. Schmidt and P. C. Paris: in *Progress in Flaw Growth and Fracture Toughness Testing*, ASTM STP 536, 1973, p. 79.
33. J. A. Vazquez, A. Morrone, and H. Ernst: *Eng. Fract. Mech.*, 1979, vol. 12, p. 231.
34. J. A. Lewis: *Fatigue Thresholds, Proceedings 1st Intl. Conf.*, Stockholm, J. Backlund, A. Blom, and C. J. Beevers, eds., EMAS Publ. Ltd., Warley, U. K., 1982, p. 1127.
35. R. O. Ritchie: *Eng. Fract. Mech.*, 1975, vol. 7, p. 187.
36. J. R. Rice: in *Fatigue Crack Propagation*, ASTM STP 415, 1967, p. 247.